

Proposed Resolution of Theory-Experiment Discrepancy in Homoclinic Snaking

W. J. Firth,¹ L. Columbo,² and A. J. Scroggie¹

¹*SUPA and Department of Physics, University of Strathclyde, Glasgow, Scotland, United Kingdom*

²*CNISM and Dipartimento di Fisica e Matematica, Università dell'Insubria, via Valleggio 11, I-22100 Como, Italy*

(Received 18 April 2007; published 7 September 2007)

In spatially extended Turing-unstable systems, parameter variation should, in theory, produce only fully developed patterns. In experiment, however, localized patterns or solitons sitting on a smooth background often appear. Addition of a nonlocal nonlinearity can resolve this discrepancy by tilting the “snaking” bifurcation diagram characteristic of such problems.

DOI: [10.1103/PhysRevLett.99.104503](https://doi.org/10.1103/PhysRevLett.99.104503)

PACS numbers: 47.54.-r, 05.65.+b, 42.65.Sf

Pattern formation is a widespread consequence of nonlinearity in spatially extended systems [1]. In simulations of model systems, a pattern typically appears spontaneously at a modulational instability (MI) threshold when a system parameter is varied. In *subcritical* cases, there is an abrupt switch into a large-amplitude pattern, which persists below the MI threshold, until collapse to the unpatterned state at a saddle-node (SN) bifurcation. A typical bifurcation diagram is shown in Fig. 1. In corresponding experiments, the expected abrupt appearance of a fully developed pattern is not always observed, however. Instead, as the driving parameter is increased, localized states (LS) [2] may appear spontaneously, multiplying as the system is driven harder and perhaps eventually merging into an extended pattern. Figure 2(a) is an example from optics, Fig. 2(b) in a gas-discharge system.

This spontaneous appearance of LS as a parameter is changed is unexpected, because in model systems, it has been proven [3] that their existence range is smaller than, and lies wholly within, the range (SN, MI) over which both patterned and unpatterned states are stable. Figure 1 is a typical example, showing a band (shaded) within which a doubly-infinite sequence of LS snakes upwards [4]. The theory of this *homoclinic snaking* is powerful and rather general [3–9]. Though it is strictly applicable only to one spatial dimension (1D), 2D systems seem to behave in a similar manner [3,10].

An obvious explanation for the discrepancy between theory and experiment is that the MI threshold varies across the system in such a way that patterns can form only at local “sweet spots.” However, an incipient pattern should not usually be confined to just those areas where the MI threshold is locally exceeded. It should invade the surrounding region, stopping only at the “locking point,” where the front between it and the unpatterned state is stationary (in Fig. 1, the right-hand edge of the shaded region). For this expansion to halt when only a single spot has formed, as in Figs. 2(a) and 2(b), would imply improbably large experimental inhomogeneities. Further, if spatial variations were indeed so strong, it becomes hard to explain the emergence at different points in Fig. 2 of near-

identical spots. Here, we suggest instead that the observed structures are indeed the LS predicted by theory, but arising beyond the MI threshold because, in addition to the short-range (quasilocal) nonlinearity responsible for pattern formation and the usual homoclinic snaking, the nonlinearity of the system has an inhibitory long-range (quasiglobal) component. This could well be due to some physical mechanism neglected in the basic theory. We discuss possible mechanisms towards the end of the Letter, but our emphasis here is on generality of effect, rather than specific models or mechanisms. If the nonlocal effect increases with the norm of the spatial structure, there would be no effect on the MI threshold, but the development of a pattern would be suppressed over some effective range. We show that such an additional nonlinearity can tilt the snakes, allowing stable LS to exist above MI, coalescing to form

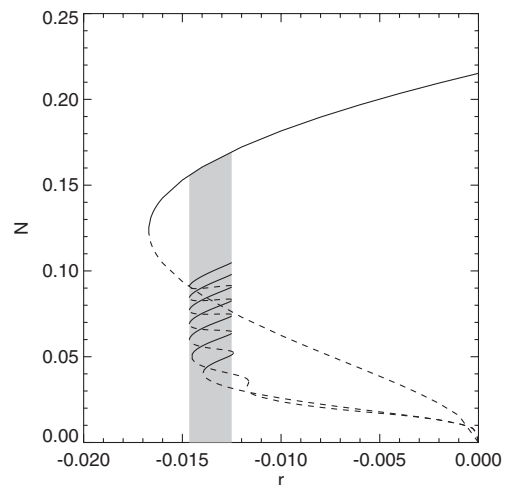


FIG. 1. Bifurcation diagram for the norm N of patterns and localized states in the quadratic-cubic Swift-Hohenberg Eq. (1) without global coupling: parameters $\nu = 0.412$, $g = 1$, $q_c = 0.5$. Domain width $L = 21 \times (2\pi/q_c) \approx 263$. Modulational instability occurs at $r = 0$. A subcritical roll pattern is shown, which exists and is stable down to a saddle-node at $r \approx -0.017$. Also shown is a pair of localized-state snakes which align with the range (shaded) over which the front between roll and trivial solutions is locked. (After [4].)

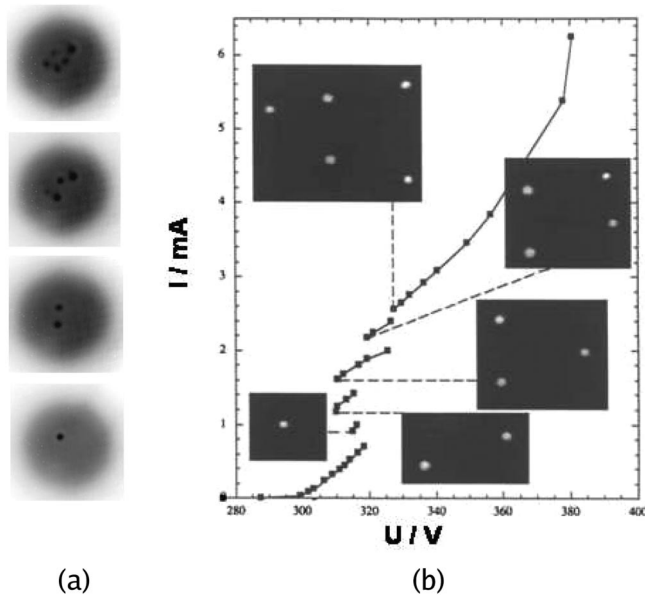


FIG. 2. (a) Sequential appearance of localized states in an optically-pumped semiconductor laser amplifier as the pumping rate is increased, leading eventually to a patternlike state [20]. (b) Diagram of current against applied potential in a gas-discharge system showing a bifurcation sequence of current filaments (courtesy of H-G Purwins [14]).

a pattern only if and when the local nonlinearity overcomes the inhibition mechanism. In the long-range (global) limit of nonlocality, we demonstrate an exact scaling law between local and local + global problems which provides an explicit proof of snake-tilting in both 1D and 2D, indicating that nonlocality may be a widely-applicable mechanism for unexpected spontaneous appearance of localized states in Turing-unstable systems. This suggests that nonlocality may resolve the anomalous experimental behavior illustrated in Fig. 2. We present detailed results for the Swift-Hohenberg equation (SHE), a standard model of pattern formation applicable to experimental systems in a wide variety of fields [1]:

$$\frac{\partial u}{\partial t} = ru - (\partial_x^2 + q_c^2)u + G_n(u) - C_{nl}u. \quad (1)$$

Here, we have added the final term, which will describe nonlocal coupling. The SHE's flat state $u = 0$ shows MI at $r = 0$ to a pattern with wave number q_c . Our main results apply exactly to all forms of SHE showing snaking, including the quadratic-cubic [4] and cubic-quintic SHE [3,7,8,11]. We have verified that similar effects arise in specific physical models, including models relevant to semiconductor lasers such as that of Fig. 2(a), but our emphasis here is on general results for generic models such as the SHE. Because Burke and Knobloch [4] give a very clear and complete description of localized states for the quadratic-cubic SHE where $G_n(u) = \nu u^2 - g u^3$, we analyze this case specifically. Pattern formation is subcritical for $\nu = 0.41$ and $g = 1$, the case analyzed in detail in

[4]: the uppermost curve in Fig. 1 represents the stable q_c -patterned state. Figure 1 also shows two sequences of LS with, respectively, even and odd numbers of peaks. Within each sequence, the energy (or other norm) characteristically “snakes” upwards, zigzagging to and fro across the locking range, adding an extra pair of peaks on each successive positive-slope “zig.” The connecting “zags” are always unstable. The LS high up each snake resemble a partial roll pattern, and their wings asymptote to the stationary fronts which characterize the locking range [4]. In this regime, the snaking can be quantified by delicate beyond-all-orders asymptotic theory [7,8].

Our interest here, however, lies with the few-peak LS forming the lower portions of the snakes, which we will term LS1, LS2, . . . by the number of peaks. To observe such LS, it should be necessary to place the control parameter within the snaking range and apply a local excitation in the form of an address pulse, causing the system to evolve onto the desired “zig” of the snake. Successful addressing has been observed in experiment, e.g., in a magnetic fluid [12] and in optical experiments, e.g., [13]. Figure 2(a) and 2(b) demonstrates a different behavior, however, in which several LS1 appear in succession, without addressing, on parameter variation. Here, snaking is either absent, or the snakes are somehow “tilted” so as to overhang the MI threshold. Figure 2(b) explicitly shows a tilted-snake bifurcation sequence in a gas-discharge experiment [14]. Bright LS1 filaments are added and subtracted essentially sequentially as the applied voltage is varied.

With a view to inducing such a tilt, we now include a finite nonlocal term in (1), setting $C_{nl} = \gamma N_K^2$, where

$$N_K^2(x) = \frac{1}{L} \int_0^L dx' K(x', x) u^2(x'). \quad (2)$$

We assume the kernel $K(x', x)$ is symmetric in its arguments. Note that if $K = 1$, the new term is global, and N_K just equals N , the rms norm of u over the system domain [4] plotted in Fig. 1. Conversely, if K is a delta function, the new term becomes local, a cubic contribution $-\gamma u^3/L$ to $G_n(u)$ in (1).

We first consider a large but finite spatial domain of size L , on which we assume $K = 1$ a good approximation. For $\gamma > 0$, the nonlocal term acts like a reduction in the drive parameter r . Indeed, for stationary states, there is an obvious but important scaling law: every stationary state $u(x; r, \gamma)$ for global coupling is an *exact* stationary state of the local Swift-Hohenberg equation for a rescaled drive parameter r . In fact, $u(x; r, \gamma) = u(x; r - \gamma N^2, 0)$. The converse is also true, so *all* stationary states of the globally-coupled Swift-Hohenberg equation (for any γ) can be found exactly, given all stationary states of the local problem. This scaling has a simple and instructive graphical implementation in (N, r) state diagrams such as Fig. 1. The states $u(x; r - \gamma N^2, 0)$ are associated with the intersections of the parabola $r' = r - \gamma N^2$ with the state curves, including the pattern curve and the snakes. In

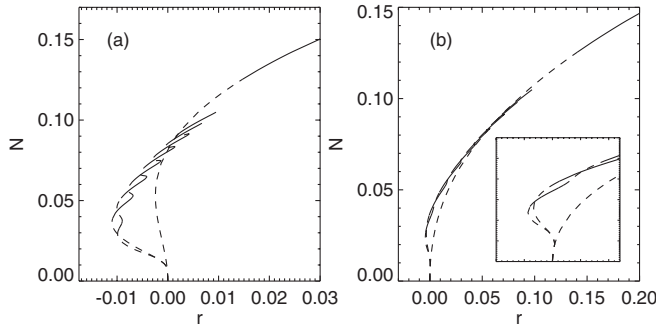


FIG. 3. Bifurcation diagram for the norm N of patterns and localized states in the quadratic-cubic Swift-Hohenberg Eq. (1) with global coupling. (a) $\gamma = 2$: The pattern range is reduced compared to $\gamma = 0$ (Fig. 1), and the snakes are tilted. (b) $\gamma = 10.0$: The pattern is now supercritical and stable only for $r > 0.14$, but both LS1 and LS2 states exist (see inset) and are stable at $r = 0$.

particular, the snakes' asymptotes (i.e., the locking range) shift to progressively higher values of r as γ is increased, tilting the snakes.

Figure 3 shows examples of global-coupling state diagrams generated by this procedure. In Fig. 3(a), for global-coupling strength $\gamma = 2$, the locking range lies above the MI threshold $r = 0$, where there are now stable LS but no stable pattern. In Fig. 3(b), $\gamma = 10$ is big enough that the pattern is supercritical at $r = 0$, but LS1 and LS2 exist subcritically and are stable. The stability assignments in Fig. 3 are derived using a Newton-Fourier method previously applied to similar problems [10,15]. From a good initial guess (here given by the scaling law), this yields both the stationary states and their spectra. The stability problems for the “global” state $u(x; r, \gamma)$ and its “source” state $u(x; r - \gamma N^2, 0)$ are different. The source states are stable on the whole of each zig of the snakes, unstable to an even mode on the whole of each “zag,” and to an odd mode on most of each zag [4]. Exact results for the even modes of the global states are lacking, but we find that stable zigs map into stable zags, consistent with the fact that the lowest-order perturbation to even-mode eigenvalues is stabilizing. However, it is easy to show that global and source states have identical odd modes, with identical eigenvalues. Since source zags map wholly or partly into global zigs, the latter can thus exhibit a novel odd-mode instability. This occurs on the LS2 branch in Fig. 3(b).

Global coupling leads to tilted snakes, as in Fig. 3, and thus to the sequential appearance of LS as the drive parameter is increased. Figure 2, however, seems to show sequential appearance of separate LS1, rather than a sequence LS1, LS2, LS3, . . . of close-packed clusters. This behavior can be captured by considering nonlocal, rather than global, coupling. The appearance of LS1 at the MI threshold persists for a kernel of range larger than the LS1 size. Figure 4 shows this for a kernel $\sim e^{-|x-x'|/\sigma}$, appropriate for a diffusive-type nonlocality [16]. Also shown in Fig. 4 is the effective r , i.e. $[r - \gamma N_k^2(x)]$, in the region

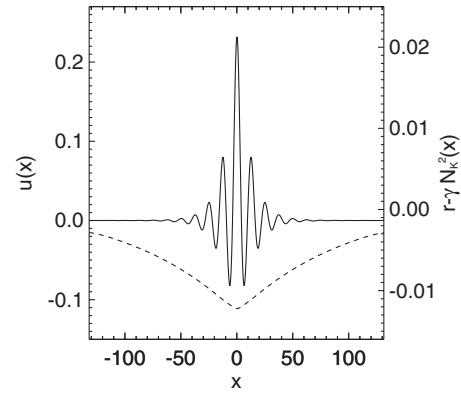


FIG. 4. LS1 (solid line) for a nonlocal exponential kernel in the quadratic-cubic Swift-Hohenberg Eq. (1), and corresponding effective r (dashed line). Parameters are $r = 0.001$, $\gamma = 12.5$, and $\sigma = 100 \approx 8 \times (2\pi/q_c)$.

surrounding the LS1. This lies below the MI threshold and thus inhibits formation of LS or patterns around the LS1. Note that the effective r at the center of Fig. 4 is close to the locking range of r in Fig. 1. This, together with the fact that the “kernel” LS1 in Fig. 4 is very similar to that predicted by global scaling, indicates that the global model is an excellent approximation to finite-range nonlocal models and thus a good basis for perturbation theory.

As well as inhibiting MI, a long-range kernel induces a long-range interaction between LS. Some insight into this can be derived from free-energy considerations. The local version of (1) has an associated free energy [4], which we write as $F(u; r, \gamma = 0)$. Adding a nonlocal term with symmetric kernel, F becomes $F(u; r, \gamma; K) = F(u; r, 0) + F_{\text{nl}}$, where

$$F_{\text{nl}} = \frac{\gamma}{4L} \int_0^L \int_0^L dx dx' K(x', x) u^2(x') u^2(x).$$

Using the properties of $F(u; r, 0)$ and the symmetry of K , it is easy to show that $F(u; r, \gamma; K)$ cannot increase during the dynamical evolution of u . It follows that all stable states of (1) are stationary, and local minima of $F(u; r, \gamma; K)$.

Suppose now that the LS1 state is given by a function $s(x)$, which is well-localized on the scale σ of K . Then the free energy for two LS1 at locations x_1, x_2 , separated by a distance of order σ or more, should take the form

$$\begin{aligned} F(u \approx s(x_1) + s(x_2); r, \gamma; K) \\ \approx 2F(s; r, \gamma; K) + f_{\text{int}}K(x_1, x_2) \end{aligned} \quad (3)$$

where we have assumed that u is well represented by the sum of two LS1 states and that $s(x)$ may be regarded as a δ function on the scale of K . Since K decreases with separation, so does the two-LS free energy, and hence there is a repulsive force acting between well-separated LS.

Combining the effective r and kernel-force concepts, and noting that both extend directly to 2D, we can envisage the following scenario beyond the MI threshold. For $r > 0$, an LS will suppress other LS throughout the zone within

which the effective r is negative (cf. Figure 4). Outside that zone, other LS can form and survive, but the kernel-induced repulsion will cause them to move apart until balanced by other forces (parameter gradients, other LS, etc.). In both 1D and 2D, this should result in the appearance of sparse populations of isolated LS with separations comparable to the kernel range. Assuming that the kernel is sharp enough at small distances to disrupt an LS n state into n LS1 states, this scenario describes Fig. 2 rather well. The kernel for a diffusive nonlocality in 2D (a Bessel function of the second kind) is singular at the origin, causing instability of higher-order nonlocal Kerr solitons [16], so disruption of dissipative LS n by nonlocality seems plausible.

Having begun the treatment of 2D systems, it is now appropriate to discuss the further applicability and extensibility of the above results to 2D, and also to more system-specific models. First, we recall that the Pomeau locking mechanism [9] is not limited to 1D, and thus the 2D snakes must also be tilted if LS are to appear spontaneously. The exact scaling between local and global problems remains exact and effective in inducing tilting in the 2D SHE. Furthermore, similar exact scaling applies to more physical models, and, in particular, to models of optical systems such as [10,17–19] relevant to Fig. 2(a) [20]. These models have at least two dynamical variables, but it is not necessary for the global effect to couple to all of them for scaling and tilting to apply. We have preliminary evidence for tilting in a cavity containing a saturable absorber [21], in which the global coupling is to the cavity tuning θ .

The choice of θ for nonlocal coupling is natural on physical grounds: thermal effects couple directly to θ since it is jointly determined by refractive index and cavity length. The temperature depends on the state of excitation of the cavity through a diffusion equation, with a spatial scale typically large compared to the LS1 size, determined by diffraction. Thermal effects thus lead naturally to the addition of a quasiglobal term to θ . Other physical mechanisms which may be responsible for nonlocality in relevant optical experiments include photocarrier diffusion and molecular orientation.

More generally, in pattern-forming systems, boundary-induced constraints typically have a quasiglobal character. Thus, the supply of energy across the system could become nonuniform through intrasystem competition in the presence of localized states. This might lead, perhaps indirectly, to mutual inhibition of LS. There may also be intrasystem competition for other resources, such as those limited by a conservation law, e.g., of material. We recently learned of independent work [22] which finds “slanted” snaking in the presence of such conservation laws.

In this Letter, we have identified a qualitative discrepancy between the theory of homoclinic snaking and related experimental observations, in that localized states commonly appear spontaneously in experiment whereas in theory they should only be accessible through hard exci-

tation. We have suggested that a competing quasiglobal nonlinearity could be responsible for this discrepancy and have given preliminary evidence in favor of our conjecture. While nonlocal nonlinearity is of great current interest in its own right [16], there has been very little work on competition between local and nonlocal nonlinearities. This competition is fundamental to the present Letter because it enables a separation between the spatial scales of the LS (determined by the critical wave vector) and their interaction (determined by the nonlocal coupling). It also permits an exact scaling for global coupling, which forms a robust basis for perturbation theory for finite-range couplings. We have proven and/or demonstrated key results on tilted snaking for the Swift-Hohenberg equation, but our approach and methods are much more widely valid and readily applicable to the sorts of experimental system in which the anomalous spontaneous appearance of localized states is observed.

This work was supported in part by the EU STREP FunFACS, and we are grateful to all partners for discussions and access to results. We thank H-G Purwins for provision of unpublished material.

-
- [1] M. C. Cross and P. C. Hohenberg, *Rev. Mod. Phys.* **65**, 851 (1993).
 - [2] *Dissipative Solitons*, edited by N. Akhmediev and A. Ankiewicz, *Lecture Notes in Physics* Vol. 661 (Springer, New York, 2005).
 - [3] P. Couillet *et al.*, *Phys. Rev. Lett.* **84**, 3069 (2000).
 - [4] J. Burke and E. Knobloch, *Phys. Rev. E* **73**, 056211 (2006).
 - [5] P. Couillet, C. Riera, and C. Tresser, *Chaos* **14**, 193 (2004).
 - [6] A.R. Champneys, *Physica D (Amsterdam)* **112**, 158 (1998).
 - [7] M.G. Clerc and C. Falcon, *Physica A (Amsterdam)* **356**, 48 (2005).
 - [8] G. Kozyreff and S.J. Chapman, *Phys. Rev. Lett.* **97**, 044502 (2006).
 - [9] Y. Pomeau, *Physica D (Amsterdam)* **23**, 3 (1986).
 - [10] J.M. McSloy *et al.*, *Phys. Rev. E* **66**, 046606 (2002).
 - [11] J. Burke and E. Knobloch, *Phys. Lett. A* **360**, 681 (2007).
 - [12] R. Richter and I.V. Barashenkov, *Phys. Rev. Lett.* **94**, 184503 (2005).
 - [13] S. Barland *et al.*, *Nature (London)* **419**, 699 (2002).
 - [14] D. Becker *et al.*, 1994 (unpublished): see also [2].
 - [15] G.K. Harkness *et al.*, *Phys. Rev. E* **66**, 046605 (2002).
 - [16] S. Skupin *et al.*, *Phys. Rev. E* **73**, 066603 (2006).
 - [17] L.A. Lugiato and R. Lefever, *Phys. Rev. Lett.* **58**, 2209 (1987).
 - [18] W.J. Firth *et al.*, *J. Opt. Soc. Am. B* **19**, 747 (2002).
 - [19] L. Spinelli *et al.*, *Phys. Rev. A* **58**, 2542 (1998).
 - [20] Y. Menesguen *et al.*, *Phys. Rev. A* **74**, 023818 (2006).
 - [21] L. Columbo *et al.* (to be published).
 - [22] J.H.P. Dawes, *SIAM J. Appl. Dyn. Syst.* (to be published).